
Title: Supercritical Fluid Extraction of Emulsions to Nanoencapsulate Vitamin E in Polycaprolactone

Author: Cristina Prieto Lourdes Calvo

PII: S0896-8446(16)30356-4
DOI: http://dx.doi.org/doi:10.1016/j.supflu.2016.10.004
Reference: SUPFLU 3773

To appear in: *J. of Supercritical Fluids*

Received date: 22-6-2016
Revised date: 6-10-2016
Accepted date: 7-10-2016

Please cite this article as: Cristina Prieto, Lourdes Calvo, Supercritical Fluid Extraction of Emulsions to Nanoencapsulate Vitamin E in Polycaprolactone, The Journal of Supercritical Fluids http://dx.doi.org/10.1016/j.supflu.2016.10.004

# Supercritical Fluid Extraction of Emulsions to Nanoencapsulate Vitamin E in Polycaprolactone

Cristina Prieto and Lourdes Calvo *

Departamento de Ingeniería Química, Facultad de Ciencias Químicas, Universidad Complutense de Madrid, Av. Complutense s/n, 28040 Madrid, Spain

crisprie@ucm.es, lcalvo@ucm.es

Correspondence should be addressed to Lourdes Calvo, lcalvo@ucm.es.

Graphical abstract

Nanocapsules of vitamin E in polycaprolactone were produced by SFEE with a high encapsulation efficiency

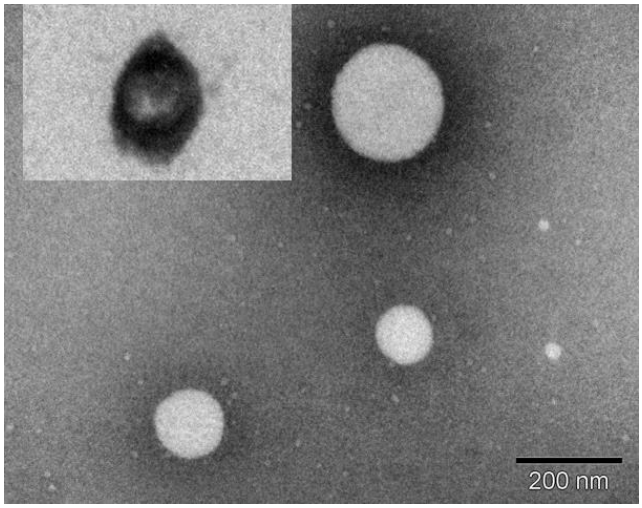

HIGHLIGHTS

- SFEE was used to nanoencapsulate Vitamin E in polycaprolactone.
- Non-aggregated core-shell spheres were obtained.
- Particle size could be finely tuned by modifying the emulsion formulation.
- Stability tests showed that particles remained unchanged over long storage periods.
- SFEE can be conducted at mild temperatures and can be easily scaled.

ABSTRACT

Supercritical fluid extraction of emulsions (SFEE) was used to encapsulate a liquid lipophilic compound, concretely vitamin E in polycaprolactone. The influence of the initial formulation on the characteristics of the nanoparticles (encapsulation efficiency, particle size distribution, and morphology) was studied. The obtained particles exhibited a high encapsulation efficiency (around 90%), narrow particle size distribution (polydispersity index between 0.24 and 0.54), and nanoscale particle sizes (between 8 and 276 nm). The morphological analysis indicated that the particles were spherical, with a core-shell structure, and non-aggregated. Operating at 8 MPa and 313 K, with a $CO_2$ flow rate of 7.2 $kg \cdot h^{-1} \cdot kg$ $emulsion^{-1}$, a low residual concentration of organic solvent (50 ppm) was obtained in 240 min at a $CO_2$ consumption of 101 kg $CO_2 \cdot kg$ $acetone^{-1}$. Stability tests indicated that the capsules remained unchanged over long storage periods (6 and 12 months).

*Abbreviations:* BPR, Back Pressure Regulator; CPF, Concentrated Powder Form; EE, Encapsulation Efficiency; FDA, Food and Drug Administration; $F_E$, Free Vitamin E Concentration; O/W, oil in water emulsion; PCL, polycaprolactone; PdI, Polydispersity Index; PGSS, Particles from Gas Saturated Solutions;

PLGA, poly(lactic-co-glycolic acid); PVA, poly(vinyl alcohol); SFEE, Supercritical Fluid Extraction of Emulsions; $T_E$, Total Vitamin E Concentration; TEM, Transmission Electron Microscopy; W/O/W, water in oil in water emulsion.

KEYWORDS: Supercritical fluid extraction of emulsions; Vitamin E; Polycaprolactone; Encapsulation; Nanocapsules.

## 1. Introduction

Vitamin E is a fat-soluble compound that exists naturally in eight different isomers including the α, β, γ and δ derivatives of tocopherol and tocotrienol [1]. Among these isomers, α-tocopherol is the most naturally abundant. It can be found in many natural sources such as wheat germ oil, sunflower seed, almond, and cereals, among others. In addition, α-tocopherol is the most important biologically active form of vitamin E, and it has exhibited antioxidant activity and the potential to modulate oxidative stress [2]. Due to its recognized virtues, α-tocopherol is widely used as a functional ingredient in food, pharmaceutical products and cosmetic preparations. However, the use of α-tocopherol is not without challenges because it is sensitive to heat and oxygen and it exhibits poor water solubility and low bioavailability [3]. A number of different α-tocopherol delivery systems have been investigated [4] as a potential means of overcoming the problems these challenge create during the processing, storage, and utilization of commercial products. These delivery systems include emulsions and nanoemulsions [3], solid-lipid nanoparticles [5], liposomes [6], and biopolymer-based micro and nanoparticles [7, 8, 9].

Of the various delivery systems that are available, biopolymer-based micro and nanoparticles can be designed to transport the bioactive to a specific site of action with

minimal degradation. The bioactive is then released in a controlled and predictable manner through a controlled degradation profile of the polymer triggered by environmental conditions such as temperature, pH, enzymes, or ionic strength [2]. An important consideration in the design of a delivery system is the need to ensure that the system effectively encapsulates the bioactive in a form that does not adversely affect product quality; for example, by altering appearance, taste, texture or stability.

Multiple processes have been developed for the formation of biopolymeric-based micro and nanoparticles [10, 11]. Some of these methods use an emulsion to produce the subsequent nanoparticles. This emulsion acts as a template that facilitates the production of particles that have a narrower particle size distribution, which is very interesting in order to have a higher degree of control over the bioactive release. However, the emulsion-based nanoparticle production processes that are currently in common use, such as solvent evaporation or solvent extraction, do not typically produce solvent-free nanoparticles [12, 13] in the submicro or nano size range that exhibit a controlled size distribution and good encapsulation efficiency. In addition, these techniques are difficult to scale [14].

Supercritical fluid encapsulation techniques promote the effective elimination of solvents thanks to the high solubility of small organic molecules on these fluids and to the fast mass transfer at low temperature and moderate pressure. Of the various supercritical fluid techniques that have been employed [15, 16], some can be used to load liquids on powders, concretely Concentrated Powder Form (CPF) and Particles from Gas Saturated Solutions (PGSS) [17]. In the case of CPF, microagglomerates with sizes of between 5 μm and 2 mm and a high liquid retention (≤ 90%) can be obtained [18]. CPF technology has been developed on an industrial scale and commercialized by the consortium of Natex,

VTP, Raps and Yara. One commercialized product that uses CPF technology is FLAVOCAPS, which consists of different flavors encapsulated in carriers such as sugar, cellulose or starch, among others. Liquid-polymer microagglomerates can be produced via the PGSS process. One example is the work of Varona et al. [19], who encapsulated lavadin oil in poly-(Ɛ-caprolactone). Particles with sizes of between 10 and 50 μm and an encapsulation efficiency of up to 50% were obtained. However, none of these techniques have been successfully employed to produce real nanocapsules (core-shell structure).

Supercritical fluid extraction of emulsions (SFEE) is a novel encapsulation technology [20, 21] that combines conventional emulsion processes with the unique properties of supercritical fluids to produce tailored micro- and nanoparticles. The basis of this process relies on the use of supercritical $CO_2$ to rapidly extract the organic phase of an emulsion, in which a bioactive compound and its coating polymer have been previously dissolved. By removing the solvent, both compounds precipitate, generating a suspension of particles in water. The produced particles have controlled size and morphology [22], due to the use of the emulsion and to the fast kinetics of the supercritical $CO_2$ extraction. Particle agglomeration in the aqueous phase is avoided since the particles are stabilized by a surfactant. In addition, this technology is very versatile. It is possible to encapsulate hydrophilic and lipophilic compounds by changing the starting emulsion. An oil in water (O/W) emulsion can be used to encapsulate lipophilic compounds, while a water in oil in water (W/O/W) emulsion can be used to encapsulate hydrophilic compounds. Previous studies have demonstrated that this process is easily scalable by means of a countercurrent column [23, 24]; however, more work should still be done on the design and optimization of the operation variables. The majority of existing research that has been conducted in this

field involved the encapsulation of solid pharmaceutical compounds in poly(lactic-co-glycolic acid) (PLGA). However, this method may also represent a promising technique for encapsulating nutraceuticals for the food industry. For example, Santos et al. [25] encapsulated β-carotene and lycopene in n-octenyl succinic anhydride (OSA)-modified starch to be used as colorants and antioxidants in the food industry.

The current study involved the use of SFEE to encapsulate vitamin E in polycaprolactone. The system for the encapsulation of this compound consisted of acetone (O) and water (W); Tween 80 was used as a surfactant, and polycaprolactone (PCL) as the encapsulating polymer. PCL is a synthetic, biocompatible, and fully biodegradable polymer, which has a semicrystalline nature (glass transition temperature of 213 K). It is approved by the FDA (Food and Drug Administration) for drug delivery. It has high hydrophobicity, high in vitro stability and is low cost. Due to its slow degradation, PCL is ideally suited for long-term delivery, or when a targeted delivery to the intestinal tract is intended [26].

The solvents used in SFEE form an emulsion with water in the presence of a surfactant but are also highly soluble in supercritical $CO_2$ at moderate pressure and temperatures. Prior to this study, previous research has examined the use of ethyl acetate [22, 24], dichloromethane [25], and acetone [23] solvents in SFEE. Acetone was selected as the organic solvent because of its low toxic potential (Class 3) which is in the line with the ICH guidelines [27].

Tween 80 was selected as the surfactant because it is a particularly attractive non-ionic surfactant that is non-toxic, environmentally friendly and biocompatible. It is commercially inexpensive and is fully approved for pharmaceutical and food use.

The aim of the current study was to examine the influence that the operational variables had on the effectiveness of the organic solvent removal. In addition, the effect of the initial formulation was assessed in order to enhance the encapsulation efficiency, particle size distribution, and morphology of the final product. Finally, the particles obtained by SFEE were compared with those obtained by conventional techniques, specifically by solvent evaporation, to evaluate the potential benefits of the use of the supercritical technology.

## 2. Materials and Methods

### *2.1 Materials*

Vitamin E (α-tocopherol, ≥95%), polycaprolactone (PCL) (MW of 10,000), Tween 80 (polyoxyethylene (20) sorbitan monooleate), acetone (≥99.5% (GC)), absolute ethanol (99.5%), sodium hydroxide (≥98%), and sodium dihydrogen phosphate monohydrate (≥98%) were all from Sigma Aldrich (Spain). Paraformaldehyde (16%), glutaraldehyde (25%), osmium tetroxide (2%), and Spurr resin were all from Electron Microscopy Sciences (USA). Uranyl acetate solution (2%) and sodium phosphotungstic acid solution (1%) were from Panreac (Spain). Acetonitrile (gradient 240 nm/ far UV HPLC grade) was from Scharlab (Spain). Carbon dioxide (>99.5%) was from Carburos Metálicos (Air Products, Spain). All materials were used as received. Millipore water was used throughout the study.

### *2.2 Preparation of the starting emulsions*

PCL and vitamin E were dissolved in acetone. The aqueous phase was prepared by dissolving the Tween 80 in water. The organic phase was added to the aqueous phase, drop by drop, and stirred on the vortex (Heidolph REAX top) for 5 min to guarantee a homogeneous dispersion.

### *2.3 Determination of phase behavior*

The first step in determining the phase behavior involved visually inspecting the samples. Samples in the whole range of composition were classified into transparent or turbid, since turbidity of colloidal dispersions is an indicator of the size of the colloid. In general terms, samples with colloids that range from 2 to 50 nm in diameter are transparent, while samples with colloid larger than 100 nm are opaque [28, 29]. All samples were analyzed in triplicate.

### *2.4 SFEE nanoparticles formation*

The SFEE apparatus consisted of a 10 ml cylindrical stainless steel extractor with a length-to-diameter (L/D) ratio of nine. Liquid chilled $CO_2$ at 263 K was delivered using a head cooled piston pump (Jasco, PU-2080). The temperature in the extractor was regulated by a heating jacket and recorded within ± 0.1 K through the use of a type T thermocouple that was positioned inside the vessel. The pressure inside the extractor was regulated by a backpressure regulator (BPR, TESCOM) and read via a digital internal pump manometer within ± 0.1 MPa and via an external online Bourbon manometer. A mass flow meter

(AlicatScientific, M-10SLPM-D) was used to measure the total amount of $CO_2$ employed. The arrangement of the equipment is shown in Figure 1.

In order to carry out the process, five grams of the freshly prepared starting formulation were placed inside the extractor before the vessel was closed. $CO_2$ was added, and the temperature was adjusted. The vessel was then pressurized to 8 MPa. Finally, the BPR was opened and the flow adjusted. The operation was deemed to be complete when the selected operation time was reached. The vessel was then slowly depressurized. A suspension of nanoparticles in water was recovered and stored in screw cap glass vials in the refrigerator until the time of analysis.

**Figure 1.**

### *2.5 Formation of nanoparticles through conventional solvent evaporation*

Acetone was extracted from the sample using two variations of the conventional solvent evaporation process. In the first, the acetone was evaporated using a mild vacuum (30 kPa) in a rotating evaporator (Rotavapor R-210, Buchi) at 323 K for 30 min, followed by a further 30 min at 6 kPa in order to concentrate the nanoparticle suspension. In the second approach, the acetone was eliminated using a hotplate with temperature control (MST Digital, Yellow Line-IKA) at 313 K for 8 h inside a fume hood under constant magnetic agitation (400 rpm).

### *2.6 Encapsulation efficiency*

The encapsulation efficiency (EE) was determined as the percentage of vitamin E entrapped in the particle. It was calculated following eq. (1).

$$Encapsulation\ efficiency\ (\%) = \frac{T_E - F_E}{T_E} \cdot 100 \quad (1)$$

The total vitamin E concentration ($T_E$) was determined after dissolving 1 ml of nanoparticles suspension in 10 ml of acetonitrile at 313 K overnight.

Free vitamin E concentration ($F_E$) was determined in the aqueous supernatant after the particles were separated by centrifugation (Digicen 21, Orto Arlesa) at 15000 rpm for 10 min.

Quantitative measurements of vitamin E (as α-tocopherol) was performed with an HPLC chromatograph equipped with a diode array detector (Jasco MD 2015) at λ=285 nm using a silica gel column (Mediterranean Sea-18, Teknokroma) as stationary phase and methanol as mobile phase at 1 ml·min$^{-1}$. The measurements were performed at 303 K. The calibration of the peak area versus concentration of α-tocopherol were linear in the concentration range of 0.175-3.500 mg·ml$^{-1}$ ($R^2$=0.9996).

The loading capacity was calculated as the mass percentage ratio between the encapsulated vitamin E and the mass of the encapsulated vitamin E plus the amount of polymer.

### *2.7 Residual concentration of organic solvent*

The amount of acetone in the nanoparticle suspension was measured using headspace gas chromatography. In order to perform the headspace, 2 ml of nanoparticle suspension were introduced into a 20 ml vial, and stabilized for 1 h at 333 K. At this temperature, the polymer melts and acetone is enriched in the vapor phase. Then, 0.5 ml of the vapor phase of this vial were extracted with a gas tight syringe and injected manually into a gas chromatograph (Shimazdu GC-2010-Plus) that was connected to a flame ionization detector. Acetone was separated using a fused-silica capillary column: 20 m long, 0.18 mm internal diameter and 0.18 μm film thickness (Zebron-ZB-1HT inferno). The oven temperature was set to 313 K for 6 minutes. The injector temperature was maintained at 453 K in split mode (ratio 19.5) and nitrogen was employed as carrier, at 7 $ml \cdot min^{-1}$ at 40.9 kPa. Each sample was measured in triplicate.

The residual concentration of acetone in the nanoparticles after the SFEE process was also measured. The aqueous suspension was centrifuged (Digicen 21, Orto Arlesa) at 15000 rpm for 10 min, to separate the pellet and the supernatant. The pellet was dried in the oven (Digitheat, Selecta) at 308 K until reaching constant weight. The dried particles were resuspended in 2 ml of milli-q water and analyzed by headspace gas chromatography following the preceding procedure.

### *2.8 Particle size distribution*

Particle size distribution was measured by photon correlation spectroscopy using a Zetasizer Nano Zs (Malvern). A dilution of the sample with milli-q water was required to achieve a suitable optical density. All measurements were performed at 298 K.

### *2.9 Nanoparticles morphology*

Aqueous suspensions of nanoparticles were centrifuged at 15000 rpm for 10 min. After that, the 70% of the supernatant was removed. A drop of concentrated aqueous suspension was negatively stained for 60 s with a 1% sodium phosphotungstic acid solution, and placed on a carbon-coated copper grid. Transmission Electron Microscopy (TEM) pictures were taken using a JEOL JEM 1010.

The internal morphology of the nanoparticles was studied by TEM using the same microscope. Samples were washed with milli-q water three times before being prepared for TEM. This procedure was performed in an Eppendorf tube, which acted as a mold. The sample preparation process [30] consisted of fixation with Karnosvky solution, washing with phosphate buffer, staining with osmium tetroxide, dehydration with absolute ethanol and inclusion in Spurr resin. After polymerization, ultrathin section of samples were cut using an ultramicrotome before being stained with uranyl salts and deposited over the TEM grid.

### *2.10 Statistical analysis*

The experiments were repeated three times. Analyses were performed in duplicate for each replicate (n=3 x 2). Means and standard deviations were calculated for all data.

## 3. Results and Discussion

This research focused on the formation of vitamin E nanocapsules using the SFEE process. First, the influence of the extraction parameters (pressure, temperature, $CO_2$ flow rate, and extraction time) was studied because these properties affect the rate at which the

acetone is removed and influence the characteristics of the product. As such, these parameters impact the technical and economic viability of the process. Then, the effect of the initial formulation was evaluated in terms of encapsulation efficiency, particle size, particle size distribution, and morphology.

### *3.1 Selection of the starting formulation*

A study of the phase behavior of the system Tween 80 / water / acetone + vitamin E + PCL at atmospheric pressure and ambient temperature was executed in order to select the composition that would be subjected to SFEE. Since the system had five components, data were plotted in a pseudoternary phase diagram, where composition of the organic phase was maintained constant (0.51% and 0.63% by mass of vitamin E and PCL, respectively). Twenty compositions that completely covered the pseudoternary phase diagram were selected. A visual observation of each sample resulted in the triangular diagram depicted in Figure 2. At high surfactant concentration (>10%), samples were transparent (shown in white) possibly due to the formation of nanosize colloids. PCL separated as a solid phase within the light shaded area.

**Figure 2.**

Only formulation 20 was turbid. Acetone is completely miscible with water; however, the presence of the vitamin E increased the viscosity of the organic phase, allowing the formation of emulsions. These emulsions were stable for days (results not shown). When

the PCL was present in the organic phase, the slow diffusion of the acetone to the water initiated PCL precipitation, due to its low solubility in acetone and insolubility in vitamin E. Thus, the turbidity of the formulation 20 was also due to the presence of the incipient particles. However, TEM images of this sample showed that particles were not completely formed at this stage and consequently they broke as shown in Figure 3. Only after the supercritical extraction of the acetone, the particles were adequately formed as described later.

**Figure 3.**

Since the colloid acts as a template, it must provide an adequate size and an O/W structure, which is required to encapsulate a lipophilic compound. These requirements were fulfilled by formulation 20, which had a composition of 71.57% of water, 28.35% of acetone, and 0.08% of Tween 80 by mass. In addition, the low concentration of surfactant in formulation 20 may favor its potential applications. This composition was also selected by Khayata et al. [31] to encapsulate vitamin E using the nanoprecipitation method coupled with solvent evaporation. This coincidence allowed us to compare the results from both techniques. Another starting mixture was selected, in this case, a transparent dispersion that corresponded with formulation 18 (80 % of water, 10% of acetone and 10% of Tween 80). Compared to formulation 20, this sample had a smaller colloid size; however, the concentration of surfactant was higher, which could condition the subsequent application of the nanoparticles.

### *3.2 Influence of the operating conditions*

Pressure and temperature have a significant effect on the emulsion characteristics and, consequently, on the produced nanoparticles. Temperature can provoke a change in the hydrophilic character of the surfactant, or even the loss of its surfactive character, if it reaches the cloud point [32].

The organic solvent should not be heated to boiling point [13] because the formation of bubbles can destroy the drops of the organic phase, affecting encapsulation efficiency, particle size, and the porosity of the polymeric wall. At atmospheric pressure, the boiling temperature of acetone is 323 K. It is also important that the glass transition temperature and the melting point of the polymer are taken into consideration because these factors can affect drug retention. Polycaprolactone is a semicrystalline polymer that has a very low glass transition temperature (213 K) and a melting point of 333 K. In addition, pressure and temperature affect the $CO_2$ density, vapor pressure of the acetone, the critical locus of the mixture $CO_2$-acetone, and the degradation of the active compound. Thus, their impact is complex and difficult to predict.

Initially, the pressure and temperature were selected such that they favored the maximum extraction rate of the organic solvent without extracting the bioactive compound while avoiding the use of high temperatures. According to the high pressure vapor-liquid equilibrium diagram of the $CO_2$-acetone mixture [33], at 8 MPa and 313 K, respectively, miscibility between carbon dioxide and acetone was complete. In these conditions, the solubility of vitamin E in supercritical $CO_2$ was quite low (0.3 mg vitamin E per g $CO_2$) [34] not being significantly improved by the presence of the acetone as no vitamin E was collected on the $CO_2$ outlet stream after many runs.

Next, the $CO_2$ flow rate was studied with the intention of maximize the extraction of the organic solvent. Several $CO_2$ flow rates were tested trying to avoid the entrainment of the sample. Table 1 shows the outcomes of $CO_2$ flow rates that varied from 1 to 3 ml·min$^{-1}$. As the results indicate, an increase in $CO_2$ flow rate led to a higher acetone extraction rate. However, the removal rate was at a maximum when the system operated at 2 ml·min$^{-1}$ (7.2 kg·h$^{-1}$·kg emulsion$^{-1}$). This can be attributed to the competing effects that arise when the $CO_2$ flow rate is augmented. On the one hand, larger flow rates enhanced Reynolds numbers and superficial solvent velocity, which benefited turbulence and external mass transfer. On the other hand, larger flow rates reduced contact time for acetone extraction.

**Table 1.**

The residual concentration of acetone versus the required amount of $CO_2$ when operating at 2 ml·min$^{-1}$ is shown in Figure 4. The extraction of the acetone was initially very fast because high amounts of acetone were available. Thus, with 12 g of $CO_2$, corresponding to a $CO_2$/acetone mass ratio of 8 kg·kg$^{-1}$, the concentration of acetone decreased from 283500 ppm to 32607 ppm (corresponding to an extraction yield of 88%) in the first 20 min. However, as the acetone concentration decreased and particles were formed, the extraction rate rapidly decreased. Some of the acetone was entrapped inside the particles and the internal diffusion and transport through the polymer wall controlled the overall rate of extraction. Consequently, higher $CO_2$ ratios and longer operation times were required to reduce the acetone concentration below 30000 ppm. For example, 50 min and a $CO_2$/acetone ratio of 21 kg·kg$^{-1}$ were required to achieve a residual solvent concentration

of 5000 ppm, which is the maximum acetone concentration permitted in pharmaceutics [27]. Operation time and $CO_2$/acetone ratio should be increased to 240 min and 101 $kg \cdot kg^{-1}$ respectively in order to achieve the maximum acetone concentration of 50 ppm required in food production [35]. At this point, acetone content in the interior of the particles was about 5 ppm. Similar extraction curve shapes were reported in [22].

**Figure 4.**

### *3.3 Influence of the composition on the characteristics of the particles*

The impact of the initial composition (amount of vitamin E, PCL, Tween 80, and acetone) on the characteristics of the nanoparticles (particle size distribution, encapsulation efficiency, and morphology) was further investigated. This stage of the research involved nine samples (A-I) that varied in respect to the amount of vitamin E, PCL, Tween 80, and acetone contained within formulation 20, which corresponds to letter A. Each effect was studied separately while the other components of the system remained constant. The nanoparticles obtained from a turbid (A) and a transparent (J) samples were compared in terms of particle size distribution and morphology. A summary of the composition of the samples (A-J) is presented in Table 2, and the influence of the composition on the nanoparticle characteristics is shown in Table 3.

**Table 2.**

As it can be observed in Table 3, the nanoparticles obtained from these formulations exhibited high encapsulation efficiency of around 90%, and a loading capacity of between 40% and 70%. In terms of particle size, they were in the nanometer range, with mean size that varied between 8 and 276 nm. In addition, they showed a fairly narrow particle size distribution, with polydispersity index (PdI) around 0.26, which increased to 0.40 or 0.54 in some samples.

The amount of vitamin E and PCL were the two formulation parameters that influenced encapsulation efficiency and consequently loading capacity. Both parameters increased as did the amount of vitamin E. This can be related to the higher initial amount of vitamin E, and to its lipophilicity [31] and viscosity [13], which prevented its leakage to the water phase. In the same way, André-Abrant et al. [36] observed that the encapsulation efficiency increased as did the drug amount for the microencapsulation of ethybenzoate in ethylcellulose by solvent evaporation. The reason of this behaviour was attributed to the increase of the organic phase viscosity, which reduced the mass transfer resistance between phases. However, the augmentation in encapsulation efficiency with increasing the amount of vitamin E is limited by the loss of stability, by pore formation or due to the insufficient thickness of the polymeric wall to protect the core [13]. For this system, the amount of vitamin E could not be further increased because the emulsion lost its stability, as evidenced by the appearance of separate vitamin E droplets.

The reduction in the amount of PCL in the range considered did not have a significant effect on encapsulation efficiency; however, loading capacity increased because of the reduction in the amount of polymer. Moreover, excessive amounts of polymer provoked a loss in stability, since phase separation and PCL precipitation were observed (results not shown). This stability loss could be linked to the low solubility of PCL in acetone. Therefore, the main parameter affecting encapsulation efficiency was the amount of vitamin E.

**Table 3.**

It is well known that viscosities of the dispersed and continuous phases together with flow-mechanic factors (agitation device, agitation intensity, time) are the most relevant parameters that affect particle size [13]. In the current study, the amount of each component was varied while the starting emulsion preparation procedure remained constant. The viscosity of the dispersed phase can be theoretically increased by rising the amount of vitamin E, PCL or reducing the amount of acetone. Surprisingly, the results in Table 3 do not respond to this tendency. In the current study, the particle size decreased as the amount of vitamin E increased, while PdI increased. Similarly, Saberi et al. [3] observed that droplet size and PdI were dependent on the amount of vitamin E acetate in an emulsion composed of vitamin E acetate, medium chain triglyceride oil, Tween 80, and water. Thus, they observed that the droplet size decreased with respect to the amount of vitamin E acetate until it reached a minimum level and then subsequently increased. With respect to PCL, it was expected that the particle size should be larger when a higher amount of PCL

was used. However, no significant changes were observed in the studied range. Khayata et al. [31] obtained the same results for the same system when using nanoprecipitation coupled with solvent evaporation. Likewise, Moinard-Checot et al. [37] did not observe any significant influence of the amount of polymer in particle size when encapsulating caprylic and capric fatty acids in PCL by emulsion-diffusion.

On the other hand, the particle size decreased as did the acetone concentration even though the viscosity of the organic dispersed phase increased. This could be due to a smaller initial colloid size caused by a lower amount of the organic phase.

A further factor that can influence particle size is the amount of surfactant. A slight increase in the amount of Tween 80 resulted in a larger particle size (compare the mean diameter of particles of samples H, A and I). The same results were obtained by Moinard-Chécot et al. [37] for the system caprylic and capric fatty acids, PCL, ethyl acetate, PVA (poly(vinyl alcohol) and water, in which the particle size increased as the concentration of PVA increased.

However, when sample J was subjected to SFEE, nanoparticles with a mean particle diameter of 8 nm were obtained; thus, particle size was highly reduced by starting from a colloid of smaller size. The increase in PdI is also noteworthy.

### *3.4 Morphology*

The morphology of the nanoparticles was studied by TEM. Particles obtained from the formulation 20 after the SFEE procedure, are shown in Figure 5A. These particles were spherical and had a size of around 200 nm. This data correlated well with the size measured

by photon correlation spectroscopy shown in Table 3. No particle agglomeration was observed.

The internal morphology of these particles was studied by cutting the nanoparticles. A cut nanoparticle of vitamin E in polycaprolactone is shown in the upper left corner of Figure 5A. As can be observed in the image, there was a hole in the interior of the nanoparticle [38] because there was no polymer inside the nanoparticle. This confirms that nanocapsules were obtained. This result can be linked to the high surface activity of the PCL, which tends to transition to the particle surface [39], generating true core-shell nanoparticles.

A TEM image of vitamin E-loaded nanoparticules obtained from the formulation 18 is shown in Figure 5B. As can be observed, by changing the starting colloid size, nanoparticle size can be highly reduced, up to 8 nm as revealed by photon correlation spectroscopy. Particles were not aggregated.

**Figure 5.**

### *3.5 Storage stability tests*

Nanoparticle suspensions obtained during these experiments were stored at 277 K in the refrigerator for 6 and 12 months. After this time, particles were reanalyzed in terms of encapsulation efficiency and particle size distribution. No significant changes were observed. The encapsulation efficiency remained constant after one year, as can be

observed in Figure 6. The same phenomenon could be observed in terms of particle size distribution and polydispersity index. This significant stability could be related to the hardness and semicrystalline character of the PCL. Furthermore, it could be associated with the fact that the high viscosity of vitamin E prevented its leakage through the pores of the PCL.

**Figure 6.**

### *3.6 Formation of nanoparticles through conventional solvent evaporation*

The vitamin E nanoparticles were formed by conventional solvent evaporation using the formulation 20 in order to compare results with those particles obtained by SFEE. The results are shown in Table 4.

**Table 4.**

The characteristics of the particles obtained by conventional solvent evaporation were similar to those obtained by SFEE when the rotatory evaporator was used at vacuum pressure; however, the residual concentration of acetone was higher (235 ppm) and the encapsulation efficiency was slightly lower (86%). The increase in the polydispersity index could be due to the acetone boiling bubbles inside the droplet, as Li et al. [13] stated. In terms of solvent evaporation at atmospheric pressure, the residual concentration of acetone

was slightly higher (157 ppm) than that observed for the SFEE procedure after the same operation time (4 h). It is important to take into account the fact that mass transfer between the water-air interface was improved using the fume hood. The characteristics of the particles were similar to those observed for the other two processes.

It is obvious that SFEE required a longer operation time than the other techniques to obtain a small sample. However, it is possible to increase the production capacity by running a continuous operation in a spray or a packed column [25, 23].

## 4. Conclusions

This research demonstrated that SFEE is a viable new method of producing nanocapsules of liquid lipophilic compounds. The particles obtained via this process exhibited a high encapsulation efficiency, narrow particle size distribution, and high storage stability. A morphological analysis confirmed that spherical, core-shell and non-aggregated nanocapsules were produced. Of the operation parameters, initial formulation had the biggest impact on nanoparticle characteristics. In contrast, the operation variables of the SFEE process had the most significant influence on the organic solvent removal. By fine tuning the pressure, temperature, and $CO_2$ flow rate, it was possible to obtain the residual solvent concentration required for food applications. Nonetheless, more work is required in this area to reduce the production costs of this approach; i.e., to reduce the operation time and $CO_2$ consumption required for the removal of the organic solvent. Above all else, it is necessary to improve the internal mass transfer that controls the overall extraction rate. However, there is little margin for improvement in terms of the manipulation of the

pressure and temperature, and the properties of the dispersed phase. Therefore, the best opportunity for this supercritical technology, involves increasing the contact time by using a packed column of adequate length, run in counter-current mode. A continuous operation would also be beneficial because it will increase the capacity of the procedure while consuming less $CO_2$, which is the most important benefit of the technology versus the conventional solvent evaporation techniques, which are difficult to scale. Furthermore, SFEE can be performed at low temperatures. This is advantageous because it is suitable for use with heat sensitive materials. Thus, future work should focus on the scale-up of the SFEE technology.

## Acknowledgments

Authors acknowledge prof. Miguel Ladero for his support on HPLC analysis, and Centro Nacional de Microscopía Electrónica (CNME) for its support on TEM analysis. Cristina Prieto thanks the Complutense University of Madrid for an UCM predoctoral grant.

## References

[1] P.M. Bramley, I. Elmadfa, A. Kafatos, F.J. Kelly, Y. Manios, H.E. Roxborough, W. Schuch, P.J.A. Sheehy, K.H. Wagner, Vitamin E, J. Sci. Food Agric. 80 (2000) 913-938, doi:10.1002/(SICI)1097-0010(20000515)80:7<913::AID-JSFA600>3.0.CO;2-3.

[2] C.M. Sabliov, C.E. Astete, Encapsulation and controlled release of antioxidants and vitamins, in: N. Garti (Ed.), Delivery and Controlled release of bioactives in foods and nutraceuticals, Woodhead Publishing Limited, Cambridge, 2008, pp. 297-330, doi:10.1016/B978-1-84569-145-5.50020-2.

[3] A.H. Saberi, Y. Fang, D.J. McClements, Fabrication of vitamin E-enriched nanoemulsions: Factors affecting particle size using spontaneous emulsification, J. Colloid Interface Sci. 391 (2013) 95-102, doi:10.1016/j.jcis.2012.08.069.

[4] M. Gonnet, L. Lethuaut, F. Boury, New trends in encapsulation of liposoluble vitamins, J. Controlled Release 146 (2010) 276-290, doi:10.1016/j.jconrel.2010.01.037.

[5] A. Dingler, R.P. Blum, H. Niehus, R.H. Müller, S. Gohla, Solid lipid nanoparticles (SLNTM/LipopearlsTM)- a pharmaceutical and cosmetic carrier for the application of vitamin E in dermal products, J. Microencapsul. 16 (1999) 751-767, doi:10.1080/026520499288690.

[6] M.N. Padamwar, V.B. Pokharkar, Development of vitamin loaded topical liposomal formulation using factorial design approach: Drug deposition and stability, Int. J. Pharm. 320 (2006) 37-44, doi:10.1016/j.ijpharm.2006.04.001.

[7] M. Otadi, F. Zabihi, Vitamin E Microencapsulation by Ethylcellulose Through Emulsion Solvent Evaporation Technique; An Operational Condition Study, World Appl. Sci. J. 14 (2011) 20-25.

[8] C.C Chen, G. Wagner, Vitamin E Nanoparticle for Beverage Applications, Chem. Eng. Res. Des. 82 (2004) 1432-1437, doi:10.1205/cerd.82.11.1432.52034.

[9] B. Albertini, N. Passerini, F. Pattarino, L. Rodríguez, New spray congealing atomizer for the microencapsulation of highly concentrated solid and liquid substances, Eur. J. Pharm. Biopharm. 69 (2008) 348-357, doi:10.1016/j.ejpb.2007.09.011.

[10] N.V.N Jyothy, P.M. Prasanna, S.N. Sakarkar, K.S Prabha, P.S. Ramaiah, G.Y. Srawan, Microencapsulation techniques, factors influencing encapsulation efficiency, J Microencapsul. 27 (2010) 187-197, doi:10.3109/02652040903131301.

[11] C.E. Mora-Huertas, H. Fessi, A. Elaissari, Polymer-based nanocapsules for drug delivery, Int. J. Pharm. 385 (2010) 113-142, doi:10.1016/j.ijpharm.2009.10.018.

[12] S. Freitas, H.P. Merkle, B. Gander, Microencapsulation by solvent extraction/evaporation: reviewing the state of the art of microsphere preparation process technology, J. Controlled Release 102 (2005) 313-332, doi:10.1016/j.jconrel.2004.10.015.

[13] M. Li, O. Rouaud, D. Poncelet, Microencapsulation by solvent evaporation: State of the art for process engineering approaches, Int. J. Pharm. 363 (2008) 26-39, doi:10.1016/j.ijpharm.2008.07.018.

[14] N. Falco, E. Reverchon, G. Della Porta, Continuous Supercritical Emulsions Extraction: Packed Tower Characterization and Application to Poly(lactic-co-glycolic Acid) + Insulin Microspheres Production, Ind. Eng. Chem. Res. 51 (2012) 8616-8623, doi:10.1021/ie300482n.

[15] M. Perrut, J. Jung, F. Leboeuf, Enhancement of dissolution rate of poorly soluble active ingredients by supercritical fluid processes Part II: Preparation of composite particles, Int. J. Pharm. 288 (2005) 11-16, doi:10.1016/j.ijpharm.2004.09.008.

[16] M.J. Cocero, A. Martín, F. Mattea, S. Varona, Encapsulation and co-precipitation processes with supercritical fluids: Fundamentals and applications, J. Supercrit. Fluids 47 (2009) 546-555, doi:10.1016/j.supflu.2008.08.015.

[17] E. Weidner, High pressure micronization for food applications, J. Supercrit. Fluids 47 (2009) 556-565, doi:10.1016/j.supflu.2008.11.009

[18] Natex Prozesstechnologie Austria, Powder Plants, http://www.natex.at/Processdescriptionpow.html, 2016 (accessed 18/03/2016).

[19] S. Varona, A. Martín, M.J. Cocero, C.M.M. Duarte, Encapsulation of Lavandin Essential Oil in Poly-(Ɛ-caprolactones) by PGSS Process, Chem. Eng. Technol. 36 (2013) 1187-1192, doi:10.1002/ceat.201200592.

[20] P. Chattopadhyay, B.Y. Shekunov, J.S. Seitzinger, R.W. Huff, Particles from supercritical fluid extraction of emulsion, U.S. Patent 2004026319 (A1), February 12, 2004.

[21] P. Chattopadhyay, B.Y. Shekunov, J.S. Seitzinger, R.W. Huff, Composite Particles and Method for Preparing, U.S. Patent 2004071781 (A1), April 15, 2004.

[22] P. Chattopadhyay, R. Huff, B.Y. Shekunov, Drug Encapsulation Using Supercritical Fluid Extraction of Emulsions, J. Pharm. Sci. 95 (2006) 667-679, doi:10.1002/jps.20555.

[23] G. Della Porta, R. Campardelli, N. Falco, E. Reverchon, PLGA Microdevices for Retinoids Sustained Release Produced by Supercritical Emulsions Extraction: Continuous

versus Batch Operation Layouts, J. Pharm. Sci. 100 (2011) 4357-4367, doi:10.1002/jps.22647.

[24] G. Della Porta, N. Falco, E. Reverchon, Continuous Supercritical Emulsions Extraction: A New Technology for Biopolymer Microparticles Production. Biotechnol. Bioeng. 108 (2011) 676-686, doi:10.1002/bit.22972.

[25] D.T. Santos, A. Martín, M.A.A. Meireles, M.J. Cocero, Production of stabilized sub-micrometric particles of carotenoids using supercritical fluid extraction of emulsions, J. Supercrit. Fluids 61 (2012) 167-174, doi:10.1016/j.supflu.2011.09.011.

[26] V.R. Sinha, K. Bansal, R. Kaushik, R. Kumria, A. Trehan, Poly-Ɛ- caprolactone microspheres and nanospheres: an overview, Int. J. Pharm. 278 (2004) 1-23, doi:10.1016/j.ijpharm.2004.01.044.

[27] Guidance for Industry QC3- Tables and List, U.S. Department of Health and Human Services, Food and Drug Administration Center for Drug Evaluation and Research (CDER), Center for Biologics Evaluation and Research (CBER), ICH, Revision 2, 2012.

[28] D.J. McClements, Nanoparticle- and Microparticle Based Delivery Systems. Encapsulation, Protection and Release of Active Compounds, CRC Press, Boca Raton, 2015, pp. 103-105, doi: 10.1201/b17280-4.

[29] J. Lyklema, Fundamentals of Interface and Colloid Science, Volume 4 Particulate Colloids, Elsevier, London, 2005, pp.2.39-2.43.

[30] J. Ayache, L. Beaunier, J. Boumendil, G. Ehret, D. Laub, Sample Preparation Handbook for Transmission Electron Microscopy. Techniques, Springer, New York, 2010, doi:10.1007/978-1-4419-5975-1.

[31] N. Khayata, W. Abdelwahed, M.F. Chehna, C. Charcosset, H. Fessi, Preparation of vitamin E loaded nanocapsules by the nanoprecipitation method: From laboratory scale to large scale using a membrane contactor, Int. J. Pharm. 423 (2012) 419-427, doi:10.1016/j.ijpharm.2011.12.016.

[32] C. Prieto, L. Calvo, Performance of the Biocompatible Surfactant Tween 80, for the Formation of Microemulsions Suitable for New Pharmaceutical Processing, J. Appl. Chem. Volume 2013, Article ID 930356, 10 pages, doi:10.1155/2013/930356.

[33] H.Y. Chiu, M.J. Lee, H.M. Lin, Vapor-Liquid Phase Boundaries of Binary Mixtures of Carbon Dioxide with Ethanol and Acetone, J. Chem. Eng. Data 53 (2008) 2393-2402, doi:10.1021/je800371a.

[34] J. Chrastil, Solubility of solids and liquids in supercritical gases, J. Phys. Chem. 86 (1982) 3016-3021, doi:10.1021/j100212a041.

[35] Spain 2011.Real Decreto 1101 /2011, de 22 de Julio, por el que se aprueba la lista positiva de los disolventes de extracción que se pueden utilizar en la fabricación de productos alimenticios y de sus ingredientes. Boletín Oficial del Estado, 30 de Agosto de 2011, 208, 94132-94137.

[36] A. André-Abrant, J.L. Taverdet, J. Jay, Microencapsulation par évaporation de solvent, Eur. Polym. J. 37 (2001) 955-963, doi:10.1016/S0014-3057(00)00197-X.

[37] D. Moinard-Chécot, Y. Chevalier, S. Briançon, L. Beney, H. Fessi, Mechanism of nanocapsules formation by the emulsion-diffusion process, J. Colloid Interface Sci. 317 (2008) 458-468, doi:10.1016/j.jcis.2007.09.081.

[38] S. Begum, I.P. Jones, C. Jiao, D.E. Lynch, J.A. Preece, Characterisation of hollow Russial doll microspheres, J. Mater. Sci. 45 (2010) 3697-3706, doi:10.1007/s10853-010-4479-3.

[39] Z.G. Tang, R.A. Black, J.M. Curran, J.A. Hunt, N.P. Rhodes, D.F. Williams, Surface properties and biocompatibility of solvent-cast poly[Ɛ - caprolactone] films, Biomaterials 25 (2004) 4741-4748, doi:10.1016/j.biomaterials.2003.12.003.

LIST OF FIGURES

**Figure 6.** Evolution of encapsulation efficiency and mean particle size of the particles obtained from formulation 20 with storage time. The columns indicate the encapsulation efficiency while the points depict the mean particle size.

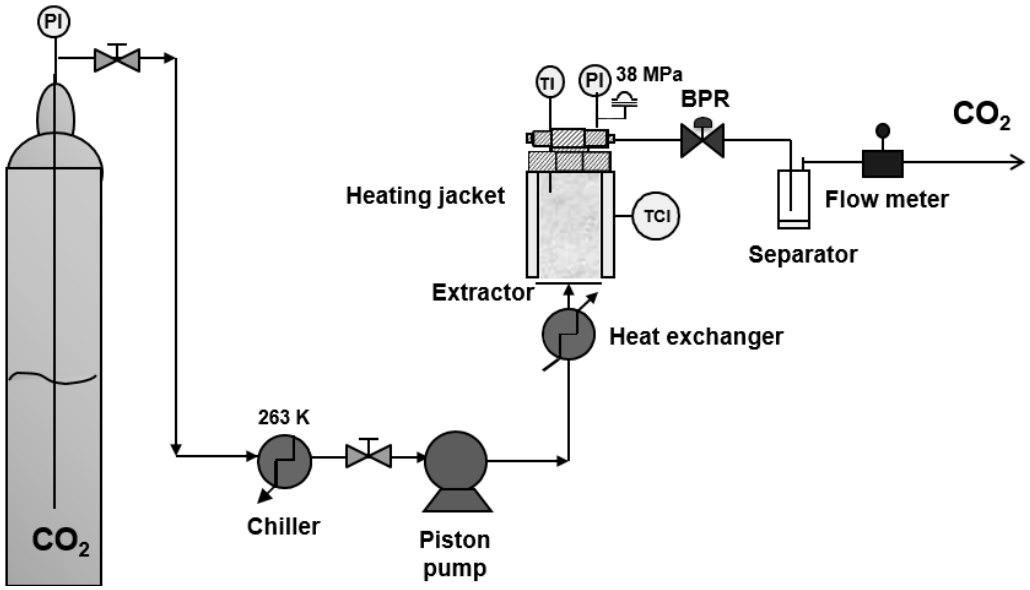


**Figure 1.**

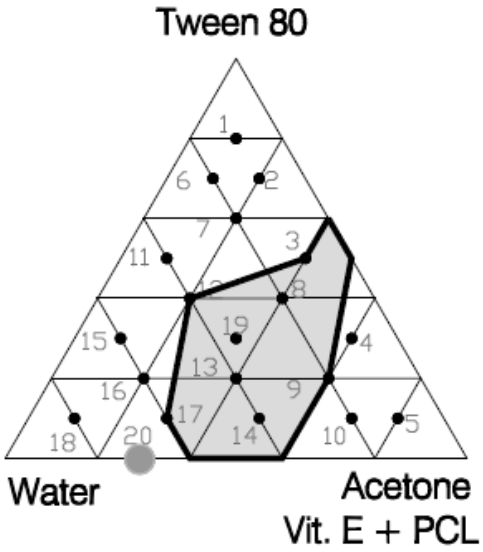


**Figure 2.**

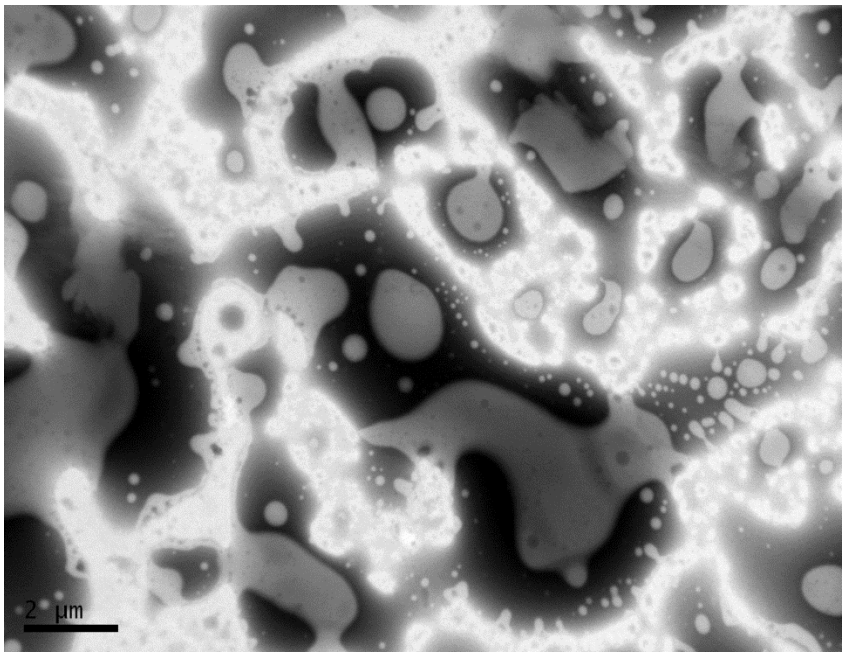


**Figure 3.**

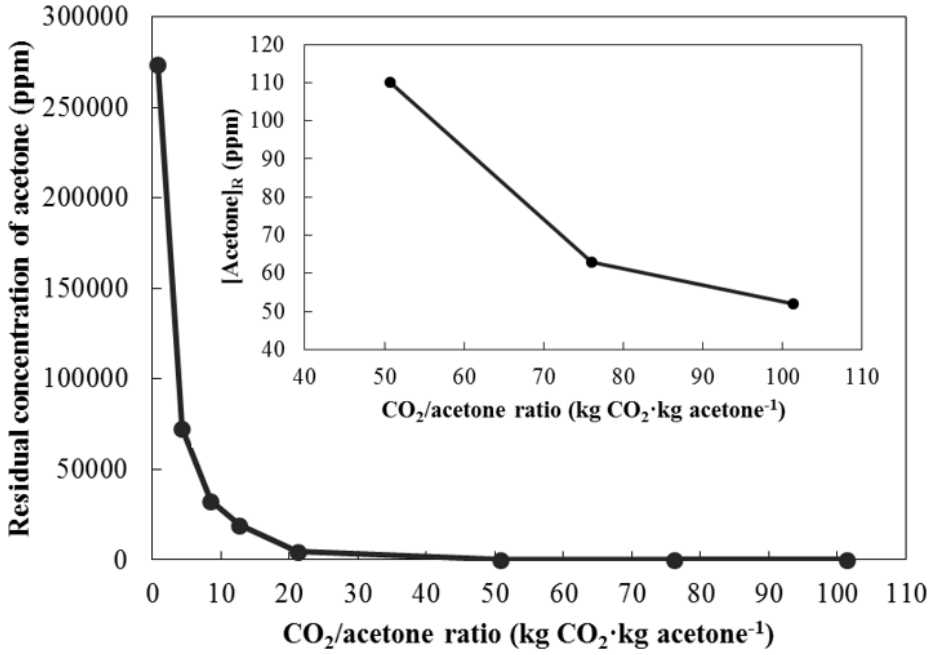


**Figure 4.**

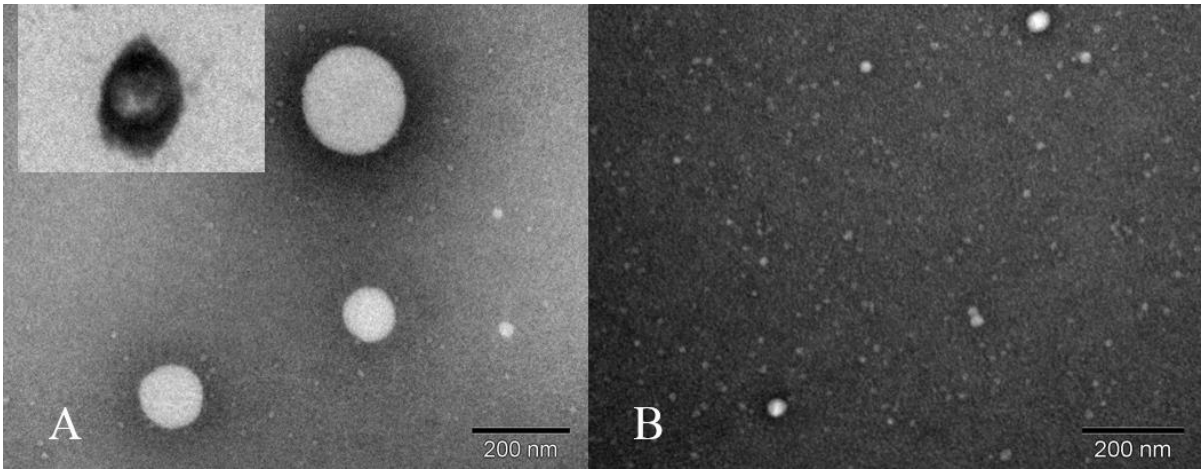


**Figure 5.**

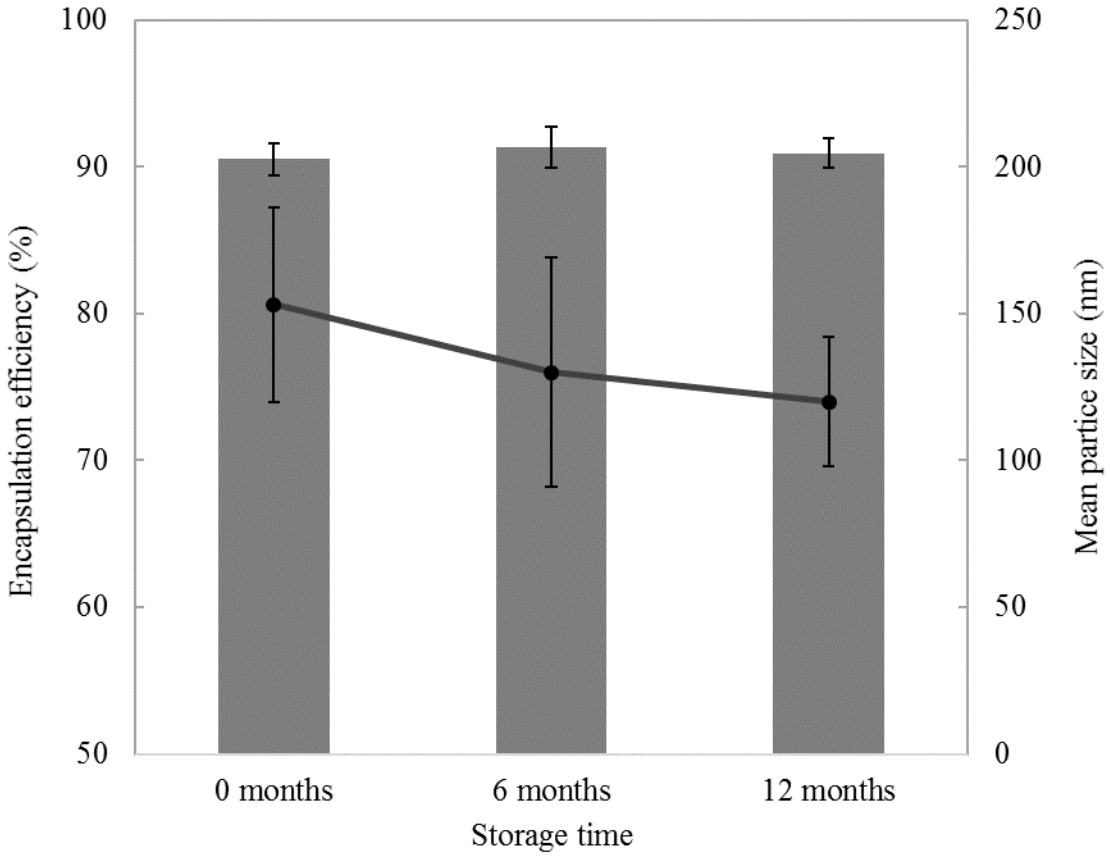


**Figure 6.**

**Table 1.** Influence of the $CO_2$ flow rate on the residual concentration of acetone. Formulation 20 had an initial acetone concentration of 28.35% by mass (283500 ppm).

| **Time** | **$CO_2$ Flow rate** | **$CO_2$/Acetone Ratio** | **Residual Concentration of Acetone** |
|---|---|---|---|
| **(min)** | **($ml \cdot min^{-1}$)** | **(kg $CO_2$·kg $acetone^{-1}$)** | **(ppm)** |
| 60 | 1 | 13 | 12380 ± 1437 |
| 120 | 1 | 25 | 4067 ± 941 |
| 180 | 1 | 38 | 2834 ± 667 |
| 30 | 2 | 13 | 19278 ± 1333 |
| 120 | 2 | 51 | 110 ± 22 |
| 180 | 2 | 76 | 63 ± 2 |
| 240 | 2 | 101 | 52 ± 7 |
| 30 | 3 | 19 | 12691 ± 1490 |
| 45 | 3 | 28 | 3427 ± 540 |
| 120 | 3 | 76 | 2066 ± 104 |

**Table 2.** Composition of the samples. Sample A corresponded to the formulation 20. Sample J corresponded to the formulation 18.

| Sample | Water | Tween 80 | Acetone | PCL | Vitamin E |
|---|---|---|---|---|---|
| | (g) | (g) | (g) | (g) | (g) |
| **A** | 3.580 | 0.004 | 1.420 | 0.009 | 0.007 |
| **B** | 3.580 | 0.004 | 1.420 | 0.009 | 0.014 |
| **C** | 3.580 | 0.004 | 1.420 | 0.009 | 0.021 |
| **D** | 3.580 | 0.004 | 1.420 | 0.003 | 0.007 |
| **E** | 3.580 | 0.004 | 1.420 | 0.007 | 0.007 |
| **F** | 4.500 | 0.004 | 0.500 | 0.009 | 0.007 |
| **G** | 4.000 | 0.004 | 1.000 | 0.009 | 0.007 |
| **H** | 3.580 | 0.002 | 1.420 | 0.009 | 0.007 |
| **I** | 3.580 | 0.050 | 1.420 | 0.009 | 0.007 |
| **J** | 4.000 | 0.500 | 0.500 | 0.009 | 0.007 |

**Table 3.** Influence of the composition on the characteristics of the nanoparticles. The variation in the amount of the compound is represented as a percentage of the total amount of starting emulsion.

| | **Effect of the Amount of Vitamin E** | | | | |
|---|---|---|---|---|---|
| **Sample** | **Amount** | **Mean diameter ± SD** | **PdI ± SD** | **EE ± SD** | **Loading capacity ± SD** |
| | **(%)** | **(nm)** | | **(%)** | **(%)** |
| A | 0.14 | 153 ± 33 | 0.26 ± 0.02 | 90.5 ± 1.1 | 42.0 ± 0.3 |
| B | 0.28 | 113 ± 51 | 0.30 ± 0.05 | 95.6 ± 2.6 | 60.1 ± 0.7 |
| C | 0.42 | 90 ± 18 | 0.40 ± 0.06 | 96.1 ± 6.4 | 69.4 ± 0.8 |
| | **Effect of the Amount of PCL** | | | | |
| **Sample** | **Amount** | **Mean diameter ± SD** | **PdI ± SD** | **EE ± SD** | **Loading capacity ± SD** |
| | **(%)** | **(nm)** | | **(%)** | **(%)** |
| D | 0.06 | 129 ± 27 | 0.24 ± 0.10 | 95.6 ± 7.0 | 69.6 ± 1.6 |
| E | 0.14 | 156 ± 19 | 0.26 ± 0.04 | 91.6 ± 6.9 | 48.5 ± 1.5 |
| A | 0.18 | 153 ± 33 | 0.26 ± 0.02 | 90.5 ± 1.1 | 42.0 ± 0.3 |
| | **Effect of the Amount of Acetone** | | | | |
| **Sample** | **Amount** | **Mean diameter ± SD** | **PdI ± SD** | **EE ± SD** | **Loading capacity ± SD** |
| | **(%)** | **(nm)** | | **(%)** | **(%)** |
| F | 9.96 | 66 ± 9 | 0.26 ± 0.01 | n.m. [1] | n.m. |
| G | 19.92 | 90 ± 12 | 0.30 ± 0.07 | n.m. | n.m. |
| A | 28.28 | 153 ± 33 | 0.26 ± 0.02 | 90.5 ± 1.1 | 42.0 ± 0.3 |
| | **Effect of the Amount of Tween 80** | | | | |
| **Sample** | **Amount** | **Mean diameter ± SD** | **PdI ± SD** | **EE ± SD** | **Loading capacity ± SD** |
| | **(%)** | **(nm)** | | **(%)** | **(%)** |
| H | 0.04 | 110 ± 27 | 0.32 ± 0.06 | n.m. | n.m. |
| A | 0.08 | 153 ± 33 | 0.26 ± 0.02 | 90.5 ± 1.1 | 42.0 ± 0.3 |
| I | 1.00 | 276 ± 10 | 0.34 ± 0.11 | n.m. | n.m. |
| | **Effect of the Initial Colloid Size** | | | | |
| **Sample** | **Amount** | **Mean diameter ± SD** | **PdI ± SD** | **EE ± SD** | **Loading capacity ± SD** |
| | **(%)** | **(nm)** | | **(%)** | **(%)** |
| A | 0.08 | 153 ± 33 | 0.26 ± 0.02 | 90.5 ± 1.1 | 42.0 ± 0.3 |
| J | 10.00 | 8 ± 1 | 0.54 ± 0.07 | n.m. | n.m. |

[1] n.m. Not measured.

**Table 4.** A comparison between the operation conditions and results obtained by SFEE and solvent evaporation at vacuum pressure or atmospheric pressure.

| | **SFEE** | **Solvent Evaporation at Vacuum** | **Solvent Evaporation at Atmospheric Pressure** |
|---|---|---|---|
| Pressure (kPa) | $8 \cdot 10^3$ | 30 + 6 | 100 |
| Operation time (min) | 240 | 30+30 | 240 |
| Temperature (K) | 313 | 323 | 313 |
| Sample amount (g) | 5 | 75 | 100 |
| Residual amount of acetone ± SD (ppm) | 52 ± 7 | 235 ± 63 | 157 ± 31 |
| Encapsulation efficiency ± SD (%) | 90.5 ± 1.1 | 86.0 ± 1.0 | 78.0 ± 1.0 |
| Loading capacity ± SD (%) | 42.0 ± 0.3 | 40.2 ± 0.1 | 37.7 ± 0.3 |
| Mean particle size ± SD (nm) | 153 ± 33 | 115 ± 15 | 123 ± 51 |
| Polydispersity index ± SD | 0.26 ± 0.02 | 0.63 ± 0.09 | 0.18 ± 0.02 |